This is an *Accepted Manuscript*, which has been through the Royal Society of Chemistry peer review process and has been accepted for publication.

Accepted Manuscripts are published online shortly after acceptance, before technical editing, formatting and proof reading. Using this free service, authors can make their results available to the community, in citable form, before we publish the edited article. We will replace this *Accepted Manuscript* with the edited and formatted *Advance Article* as soon as it is available.

You can find more information about *Accepted Manuscripts* in the **Information for Authors**.

Please note that technical editing may introduce minor changes to the text and/or graphics, which may alter content. The journal's standard **Terms & Conditions** and the **Ethical guidelines** still apply. In no event shall the Royal Society of Chemistry be held responsible for any errors or omissions in this *Accepted Manuscript* or any consequences arising from the use of any information it contains.

(A) Formation of liquid microcapsules using WPI-GA complex coacervates

(B) Drying

Spray dried   Freeze dried

(C) Oxidative stability
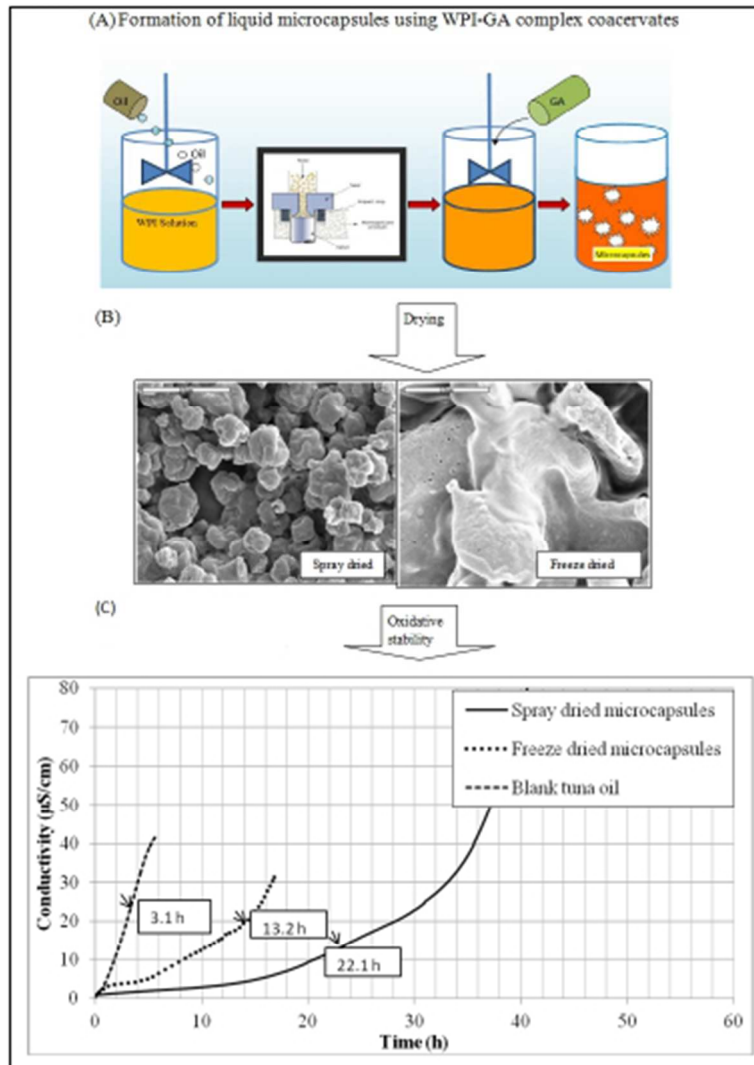
101x142mm (96 x 96 DPI)

1   **Complex coacervation with whey protein isolate and gum Arabic for the**

2   **microencapsulation of omega-3 rich tuna oil**

3   Divya Eratte[1], Bo Wang[3], Kim Dowling[1], Colin. J. Barrow[3], and Benu .P. Adhikari[2*]

4   [1]School of Health Science, Federation University Australia, Mount Helen, VIC 3353,

5   Australia

6   [2]School of Applied Science, RMIT, Melbourne, VIC, 3001, Australia

7   [3]Centre for Chemistry and Biotechnology, Deakin University, Geelong, VIC 3217,

8   Australia

9   **ABSTRACT**

10   Tuna oil rich in omega-3 fatty acids was microencapsulated in whey protein isolate

11   (WPI)-gum Arabic (GA) complex coacervates, and subsequently dried using spray and

12   freeze drying to produce solid microcapsules. The oxidative stability, oil

13   microencapsulation efficiency, surface oil and morphology of these solid microcapsules

14   were determined. The complex coacervation process between WPI and GA was

15   optimised in terms of pH, and WPI-to-GA ratio, using zeta potential, turbidity, and

16   morphology of the microcapsules. The optimum pH and WPI-to-GA ratio for complex

17   coacervation was found to be 3.75 and 3:1, respectively. The spray dried solid

18   microcapsules had better stability against oxidation, higher oil microencapsulation

19   efficiency and lower surface oil content compared to the freeze dried microcapsules. The

* **Corresponding author: Tel: +61 3 992 59940   Fax:+61 3 992 53747   benu.adhikari@rmit.edu.au**

20   surface of the spray dried microcapsules did not show microscopic pores while the

21   surface of the freeze dried microcapsules was more porous. This study suggests that solid

22   microcapsules of omega-3 rich oils can be produced using WPI-GA complex coacervates

23   followed by spray drying and these microcapsules can be quite stable against oxidation.

24   These microcapsules can have many potential applications in the functional food and

25   nutraceuticals industry.

26

27   Keywords: Omega-3 fatty acids, Microencapsulation, Complex Coacervation, Whey

28   protein isolate, Gum Arabic, Spray drying, Freeze drying

29

30

31

32

33

34

35

36

37

38

39

1. Introduction

40

41   The health benefits associated with the consumption of omega-3 fatty acids are well

42   known, particularly for maintaining normal brain function[1], reducing the risk of cancer[2]

43   and preventing cardiovascular disease.[3] The lower actual versus recommended daily

44   intake (RDI) of omega-3 fatty acids in many countries has been the major driving force

45   for the development of functional foods and nutraceuticals containing eicosapentaenoic

46   acid (EPA, C20:5n3) and docosahexaenoic acid (DHA, C22:6n3). Fish oil is the major

47   source of EPA and DHA for fortified foods and nutritional supplements.[4,5] However, fish

48   oils are highly susceptible to oxidation due to the highly unsaturated structure of long-

49   chain omega-3 fatty acids. Oxidation of polyunsaturated fatty acids (PUFAs) produces

50   peroxides and other harmful secondary oxidation products, which ultimately decreases

51   the nutritional value of omega-3 fatty acids and negatively impacts the sensory

52   properties.[6,7] Hence, the need for omega-3 rich oils to be microencapsulated in suitable

53   wall materials to preserve their nutritional and organoleptic quality is ascertained.[8,9]

54   Complex coacervation is a liquid-liquid phase separation phenomenon that occurs when

55   electrostatically opposite charged biopolymers are brought together under certain specific

56   conditions.[10] Barrow et al.[11] reported that it is one of the most effective methods of

57   microencapsulating omega-3 fatty acids rich oils, primarily using gelatine as the wall

58   material. Broadening the range of suitable wall material for the microencapsulation of

59   omega-3 fatty acids is important for expanding the scope and applicability of this

60   important technique. Hence in the present study we explored the process of complex

61   coacervate formation between cationic whey protein isolate and anionic gum Arabic to

62   microencapsulate tuna oil which is rich in omega-3 fatty acids. WPI is a by-product of the

63   dairy industry and it has been widely used in the food processing industry due to its

64   nutritional qualities and unique physio-chemical properties such as emulsion stabilization

65   and gel formation.[12] As a natural protein, WPI exhibits positive charge below its

66   isoelectric point (IEP). WPI is effective in lowering interfacial tension at the oil-water

67   interface, quite promptly migrates to the interface from bulk solution, and possesses good

68   skin forming ability when it is dried.[13] GA is a composite edible polysaccharide which

69   shows a negative charge above pH 2.2.[14] It is one of the most commonly used stabilizers

70   in the food and pharmaceutical industries.[15] GA mainly consists of six carbohydrates

71   moieties and less than 2% proteins.[16,17] Hence, complex coacervation between WPI and

72   GA can occur by adjusting the pH and the WPI-to-GA ratio of their mixture.

73   However, there are only limited studies on the microencapsulation of oils using WPI-GA

74   complex coacervates. Weinbreck et al.[18] encapsulated sunflower oil, lemon and orange oil

75   flavours with WPI-GA coacervates. However, this work did not proceed to produce dried

76   microcapsules and was confined in producing liquid microcapsules. Zhang et al.[19]

77   investigated the encapsulation of fish oil using WPI-GA complex coacervates. This work

78   focussed mainly on studying the effect of different GA and WPI types in forming

79   complex coacervates and microcapsules. So far, the optimization of complex

80　　coacervation process between WPI and GA aiming to better microencapsulate omega-3

81　　rich oils has not been systematically studied.

82　　Dried microcapsules produced through complex coacervation could offer omega-3 rich

83　　oils better shelf-life and wider applicability.[20] Both spray and freeze drying are

84　　commonly used in the food industry to produce powder or solid microcapsules. However,

85　　the application of different drying techniques can influence the stability and other

86　　characteristics of powdered microcapsules even at the same optimal complexation and

87　　emulsification conditions. For example, the freeze dried products are more porous due to

88　　the sublimation while spray dried powders containing biopolymers are usually irregular

89　　and contain surface folds.[21,22] However, the effect of spray and freeze drying processes

90　　on the microencapsulation efficiency, surface oil and oxidative stability of solid

91　　microcapsules produced using WPI-GA complex coacervates is poorly understood.

92　　In this context, there were three key objectives in this study. Firstly, to determine the

93　　optimum process parameters at which complex coacervation between WPI and GA can

94　　occur. Secondly, to produce and characterise the liquid microcapsules of omega-3 rich

95　　tuna oil produced by using these WPI-GA complex coacervates as the shell of the

96　　microcapsules. Finally, to produce and characterise spray and freeze dried solid

97　　microcapsules in terms of oxidative stability, microencapsulation efficiency, and surface

98　　oil content and morphological analysis through scanning electron microscopic (SEM)

99　　examinations.

100   **2. Materials and methods**

101   **2.1 Materials**

102   Whey protein isolate (WPI 895[TM]) was donated by Fonterra Cooperative, New Zealand.

103   Gum Arabic was purchased from Sigma-Aldrich Ltd (New South Wales, Australia). Tuna

104   oil (HiDHA), containing 39.03% omega-3 fatty acids (Table 1), was a gift from NuMega

105   Ingredients Ltd. (Victoria, Australia) and stored at 4 ^{o}C until use. All other chemicals

106   were purchased from Sigma–Aldrich Australia (New South Wales, Australia) and were of

107   analytical grade and used without further purification.

108   **2.2 Optimization of the complex coacervation process**

109   The zeta potential, yield of complex coacervates and turbidity data were used to

110   determine the optimum pH and WPI-to-GA ratio for the formation of complex

111   coacervates.

112   **2.2.1 Optimization of pH**

113   Zeta potential values as a function of pH were used to determine the optimal pH range at

114   which complex coacervation between WPI and GA was formed. Zeta potential values for

115   WPI (1.5% w/w) and GA (0.5% w/w) were measured in the pH range of 3.0 -7.0 at 25°C

116   by using a zetasizer (Zetasizer NanoZS 90, Malvern Instruments Ltd. Worcestershire,

117   WR14 1XZ, UK), which determines the electrophoretic mobility and then calculates the

118   zeta potential using appropriate conversion equations.[23,24]

119   The absorbance of the mixture of WPI (0.1%) and GA (0.03%) was measured within

120   3.0-5.0 pH range using a UV spectrophotometer (UV-1800, Shimadzu, Kyoto, Japan) at

121   750 nm. The absorbance (or turbidity) of WPI (0.1%, w/w), GA (0.03%, w/w), and the

122   mixture of WPI and GA at different ratios, were measured at 750 nm. The pH value at

123   which the maximum absorbance (turbidity) was observed was considered the optimal pH

124   for complex coacervation between WPI and GA.

125   **2.2.2 Optimization of the WPI-to-GA ratio**

126   The turbidities of various mixtures of WPI and GA at different ratios (1:1, 3:1, 3:2, 4:1

127   and 5:1) were determined using the light absorbance of these mixtures at 750 nm using a

128   UV spectrophotometer as detailed above.

129   The optimum WPI-to-GA ratio which resulted in the highest coacervation yield was also

130   measured. For this purpose, aqueous dispersions containing WPI and GA at the above

131   mentioned ratios were prepared at ambient temperature and the pH of these dispersions

132   was adjusted to the optimum value (Section 2.2.1). These pH adjusted dispersions were

133   allowed to stand for 5 h to facilitate the precipitation of the gel-like complex coacervates.

134   Then, the coacervates were carefully separated and dried at 105° C until a constant mass

135   was reached. The coacervate yield was then calculated by using equation (1) given

136   below.

137   Coacervate yield (%) = $\dfrac{\text{Mass of the dried coacervates (g)}}{\text{Total mass of WPI+GA used (g)}}$ (1)

138   **2.3 Confocal laser scanning microscopic (CLSM) analysis**

139   The microstructure of tuna oil microencapsulated with WPI-GA using complex

140   coacervation at various pH was observed using a CLSM (Eclipse Ti, Nikon, Japan). WPI

141   and GA were covalently labelled with fluorescein 5-isothiocyanate (FITC) and

142   rhodamine B-isothiocyanate (RITC), respectively. Tuna oil was physically labelled with

143   Bodipy-X-Azide. Briefly, FITC solution (10 mg/100 ml ethanol) and RITC solution

144   (10 mg/ 100 ml water) were prepared separately. Then 50 ml of FITC solution and 50 ml

145   of RITC solution were used for the preparation of WPI (3%) and GA (1%) solutions and

146   the microencapsulation procedure was carried out as per Section 2.4. Covalent labelling

147   of WPI and GA was done in order to visualize these biopolymers in the mixture. A lens

148   with 40 X magnification and a laser with an excitation wavelength of 645 nm (for

149   Bodipy-X- Azide), 488 nm (for FITC) and 561nm (for RITC) were used.

150   **2.4 Microencapsulation of tuna oil**

151   Firstly, 250 ml WPI solution (3%, w/w) was prepared at ambient temperature and 15 g of

152   tuna oil was dispersed in this solution. The mixture was stirred using a mechanical stirrer

153   (IKA® RW 20 digital overhead stirrer, Germany) at 800 rpm for 10 min and was further

154   homogenized using a microfluidizer at 45 MPa for 3 passes (M110L, Microfluidics,

155   Newton, USA) to produce an O/W emulsion. Then 250 ml GA solution (1%, w/w) was

156 added drop wise into this O/W emulsion and was stirred at 800 rpm. The pH of this

157 emulsion was then adjusted to 3.75 by adding 1% citric acid drop wise in order to induce

158 electrostatic interaction between WPI and GA. The microencapsulation procedure was

159 carried out at 25° C, followed by cooling to 5° C at a rate of 5° C/h using a programmable

160 water bath (PolyScience, Niles, Illinois, USA). A microscope (Eclipse 80 i, Nikon, Japan)

161 was used to obtain optical images of the coacervates microcapsules. The morphology of

162 the microcapsules was captured as a function of pH and temperature. Finally, the

163 microcapsules were dried to produce solid or powder microcapsules.

164 **2.5 Drying of coacervate microcapsules**

165 A portion of suspension containing microcapsules produced as per Section 2.4 was spray

166 dried (Mini spray dryer B-290, BÜCHI Labortechnik, Switzerland) using inlet and outlet

167 temperatures of 180° C and 80 ± 3 ^{o} C, respectively. The powdered microcapsules were

168 collected and stored in an air tight desiccator for further characterization.

169 The second portion of the liquid microcapsules was frozen at -20° C overnight and was

170 freeze dried (Christ Alpha 2-4LD, Osterode, Germany). The temperature of the ice

171 condenser was set at -50^0 C and the vacuum pressure was set to 0.04 mbar. The frozen

172 samples were dried for 30 hrs and the dried product was collected, pulverized and stored

173 in an air tight desiccator for further tests.

174 **2.6 Physicochemical properties of the microcapsules**

9

175 **2.6.1 Oxidative stability**

176 Accelerated oxidation tests were carried out for the liquid oil and the solid or powdered

177 microcapsules using a Rancimat (model 743, Metrohm, Herisau, Switzerland).[25] Four ml

178 tuna oil or 1.5 g dried microcapsule powder was heated at 90°C under purified air (flow

179 rate of 20L/h). Briefly, when the oxidation of oil takes place, the conductivity of Milli-Q

180 water in the collection chamber increases due to the entrapment of the volatile products

181 (formic acid) and this increase is plotted by the accompanied software (Rancimat

182 Control, version 1.1,Metrohm, Herisau, Switzerland). Then the *OSI* value of the samples

183 is graphically determined by locating tangential intersection point on experimental data

184 as described by Läubli et al, 1986.[26] The induction time (at which the conductivity of

185 sample increases sharply due to oxidation) of the test sample was recorded and used as

186 the oxidative stability index (*OSI*). Analyses were performed in duplicate.

187 **2.6.2 Microencapsulation efficiency**

188 Microencapsulation efficiency was calculated by measuring the surface oil (solvent

189 extractable) and total oil of the microcapsules. Surface oil was determined by the washing

190 method described by Liu et al.[27] with slight modification. Three grams of dried

191 microcapsule sample was dispersed in 30 mL isohexane and this was shaken at 225rpm

192 for 5 minutes on an orbital shaker (Stuart SSL-1, Carl Roth, Karlsruhe, Germany). The

193 slurry was then filtered through filter paper (Whatman, 5µm) and the solid particles

194   caught on the filter were further washed three times with 10 ml of isohexane in each

195   wash. The filtrate was dried under nitrogen followed by drying at 100° C for 1h in an

196   oven. The sample dried in this way was placed in a fume hood overnight to remove the

197   residual solvent. The surface oil content was then measured gravimetrically.

198   The total oil content in the dried microcapsules was determined by an acid digestion

199   method using 4N HCl. Three grams of powdered microcapsule sample was dispersed in

200   30 ml of 4N HCl and shaken at 225 rpm for 15 minutes on an orbital shaker (Stuart SSL-

201   1, Carl Roth, Karlsruhe, Germany) in order to dissolve the shell materials. Fifteen ml of

202   isohexane was added to this mixture and then shaken for 18 h at ambient temperature to

203   extract the oil. The mixture was centrifuged at 24,471 g at 20°C for 30 minutes. The

204   hexane phase containing the dissolved oil was collected and dried by nitrogen under fume

205   hood. This partially dried sample was further dried at 100°C in an oven and then placed

206   under a fume hood to remove the residual solvent. The oil content was then determined

207   gravimetrically.

208   The percent surface oil (SO), total oil (TO) and microencapsulation efficiency (ME) were

209   calculated using equations (2), (3) and (4), respectively.

210      $$SO = \frac{W_s}{W_m} \times 100\% \quad (2)$$

211      $$TO = \frac{W_t}{W_m} \times 100\% \quad (3)$$

212 $$ME = \frac{w_t - w_s}{w_t} \times 100\% \quad (4)$$

213 where w_t and w_s are the mass values (g) of total and surface oil of the microcapsules and

214 w_m is the mass (g) of the microcapsules.

2.7 Surface morphology of the solid microcapsules

216 A Scanning Electron Microscopy (JEOL JSM6300 SEM, Tokyo, Japan) was used to

217 acquire the morphology of dried microcapsules. Samples were lightly gold sputter coated

218 (Sputter coater, Agar Aids, England) for 45 seconds and imaged under scanning electron

219 microscope operated at 7kV and low beam current.

2.8 Statistical Analysis

221 All measurements were performed at least in triplicates and the results are reported as

222 mean± standard deviation. The SPSS statistical package (Version 21, Lead Technologies,

223 USA) was used for the analysis of variance (ANOVA) to determine whether or not

224 significant difference existed between two mean values. The confidence level of 95%

225 $(p<0.05)$ was used.

3. Results and discussion

3.1 Optimal parameters for complex coacervation between WPI and GA

3.1.1 Optimal pH for complex coacervation

229   The zeta potentials of WPI and GA within the pH range of 3.0 - 7.0 are presented in Fig.

230   1A. The zeta potentials of WPI within this pH range varied from positive (16.80 mV at

231   pH 3.0) to negative (-20.21 mV at pH 7.0). The isoelectric point (IEP) at which the zeta

232   potential becomes zero was found to be 4.4, which is in agreement with previous

233   reports.[28] The zeta potential of GA is always negative independently of pH due to

234   carboxylate groups being the only charged functionalities present in its globular-like

235   random coil structure.[29] If at least one of the macromolecules in a mixture is not a strong

236   polyelectrolyte, then coacervation is likely to occur.[30] Therefore, it can be inferred from

237   the Fig. 1A that the pH at which complex coacervation between WPI and GA will occur

238   is at or below pH 4.4.

239   The turbidity test (Section 2.2.1) was carried out within the pH range of 3.0 -5.0 in order

240   to locate the optimum pH value for complex coacervate formation. The absorbance

241   values of the WPI and GA mixed dispersions are presented in Fig. 1B. As can be seen

242   from this figure, formation of dense complex coacervates occurred within the pH range

243   and formation of the complex coacervates was greatest at pH 3.75. Hence this pH value

244   was chosen as the optimum pH for complex coacervate formation.

245   **3.1.2 Optimal WPI-to-GA ratio for complex coacervation**

246   The ratio of protein to polysaccharide in the mixture influences the charge balance of

247   polyions and consequently their complexation behaviour.[31] Based on the work described

248   in the previous section (Section 3.1.1) we used the optimum pH of 3.75 to study the

13

249   binding between WPI and GA. As can be seen from Fig. 2A, the highest absorbance

250   value was observed at a WPI-to-GA ratio of 3:1, which is due to the highest level of

251   turbidity caused by the electrostatic interaction between WPI and GA. To corroborate this

252   data, the yield of complex coacervates was measured (Section 2.2.2) at different WPI-to-

253   GA ratios and the data is presented in Fig. 2B. The highest coacervate yield of 71.26 %

254   was obtained at the WPI-to-GA ratio of 3:1, which corroborates the turbidity data

255   (Fig.2A). Other WPI-to-GA ratios produced lower coacervate yields, possibly due to the

256   formation of soluble rather than insoluble complexes occurring when either of the

257   biopolymer is in excess. Soluble complexes are formed due to the charge imbalance and

258   produce weaker electrostatic interaction, which results in lower coacervate yield.[31] The

259   biopolymer ratio and dispersion pH are known to alter the charge density of the

260   complexes.[23] At pH 3.75 and WPI-to-GA ratio of 3:1, the electrostatic interaction

261   between WPI and GA resulted in two phases specifically due to the formation of a soft

262   dense coacervate phase rich in biopolymers and a dilute phase poor in biopolymer

263   concentrations. Hence, this WPI-to-GA ratio of 3:1 was selected as the optimum ratio to

264   produce complex coacervates.

265   **3.2 Observation of microcapsule formation**

266   Optical microscopy was used to study the formation of complex coacervates and their

267   subsequent absorption onto oil droplets. As can be seen from Fig. 3A, 3B and 3C, no

268   obvious complex coacervates were absorbed onto the oil droplets above pH 5.0. When

269   the pH was further lowered to 4.5 (close to the IEP of WPI), the aggregation of oil

270   droplets was observed (Fig. 3D). This may be due to weaker repulsion between

271   negatively charged WPI and GA when the surface charge of WPI approaches neutral

272   (Fig. 1A). Also, the steric repulsion between droplets was not enough to overcome the

273   aggregation of the droplets. In this environment, the attractive interactions between the

274   biopolymer molecules, such as van der Waals and hydrophobic, become dominant.

275   Kulmyrzaev et al.[32] reported that excessive droplet aggregation occurs when the net

276   charge on the droplet doesn't generate stronger electrostatic repulsive force than the

277   strength of the attractive forces in the emulsion. It can be observed from Fig. 3E to 3H

278   that when the pH of the dispersion was lowered below the isoelectric point of WPI (IEP =

279   4.4), complex coacervation occurred in the surrounding continuous phase, and these

280   coacervates migrated to the surface of the oil droplets, and formed a coacervates layer. It

281   was observed that complex coacervation occurred and aggregation of the oil droplets

282   started to take place below pH 4.4. This is because WPI became positively charged below

283   its IEP and electrostatic attraction with negatively charged GA started to occur. Finally, a

284   smooth layer of WPI-GA complex coacervates was formed uniformly around the oil

285   droplets (Fig. 3G) at pH 3.75, which is consistent with the turbidity and coacervate yield

286   data (Fig.1B and Fig. 2A, 2B).

287   When the liquid microcapsules were cooled from ambient temperature to 5°C, the "free

288   coacervates" which remained suspended in the continuous phase (at ambient temperature)

15

289 began to absorb onto the surface of the aggregated oil droplets (Fig. 3H). This implies

290 that cooling is an important step in stabilizing oil emulsions using complex coacervates.

291 As can be seen from Fig. 3H, multicored microcapsules were formed due to the formation

292 of WPI-GA complex coacervates. This may be partly due to homogenization occurring

293 under high pressure when using a microfluidizer. Yeo et al.[33] reported that single core

294 microcapsules were produced when a lower degree of homogenization was used while

295 multi core microcapsules were produced under a higher degree of homogenization.

296 Confocal laser scanning microscopy (CLSM) was used to visualize complex coacervate

297 formation between WPI and GA and to confirm the optimized processing conditions (pH

298 3.75 and WPI-to-GA ratio 3:1) and also to assess whether tuna oil droplets were

299 microencapsulated in the WPI-GA complex coacervates. WPI (labelled green) and GA

300 (labelled red) in the dispersion before complex coacervation are shown in Fig. 4A and

301 Fig. 4B. These figures are similar to the optical micrographs of dispersion before

302 complex coacervation (Fig. 3A). WPI and GA are clearly visible in the complex

303 coacervate as shown in Fig. 4C and Fig. 4D, respectively. The micrograph presented in

304 Fig. 4C is WPI-GA complex coacervate (labelled WPI (green) only) formed under the

305 optimized processing conditions. Similarly, Fig. 4D is the WPI-GA complex coacervate

306 (labelled GA (red) only) formed under the same optimized conditions. Fig. 4E shows that

307 WPI-GA complex coacervate (yellow in colour) was formed at pH 3.75 and at a WPI-to-

308 GA ratio of 3:1, and neither WPI (green colour) nor GA (red colour) is dominant in Fig.

16

309   4E, indicating that complex coacervation has occurred between WPI and GA under the

310   processing conditions used. These CLSM images are consistent with the optimum

311   conditions for formation of complex coacervates between WPI and GA being pH 3.75

312   and a WPI-to-GA ratio of 3:1.

313   Multiple labelling CLSM was used to visualize the distribution of tuna oil droplets

314   (labelled blue) in the WPI-GA microcapsules (Fig. 5). Microcapsules without and with

315   visualisation of oil droplets are shown in Fig. 5E and Fig. 5F, respectively, to assess

316   whether complexation has occurred between WPI and GA at pH 3.75 and at the WPI-to-

317   GA ratio of 3:1, and also to confirm the distribution of oil droplets in the microcapsules.

318   The GA component in the microcapsule is shown in Fig. 5A (GA labelled red), the WPI

319   component in Fig. 5B (WPI labelled green), and oil in Fig. 5C (oil droplets labelled blue).

320   The mixture of oil, WPI and GA in the dispersion before carrying out complex

321   coacervation process is presented in Fig. 5D. It can be clearly seen from Fig. 5D that no

322   complex coacervates of WPI and GA was formed and oil droplets were just dispersed in

323   the mixture at pH 6.0. An obvious formation of WPI-GA complex coacervate (yellow)

324   and distribution of oil droplets in the coacervate can be clearly seen in Fig. 5E and Fig.

325   5F. The Z-average size of the oil droplets was 223.0 nm (polydispersity index (PdI) =

326   0.376) and these oil droplets are clearly microencapsulated in the WPI -GA matrix.

327   **3.3 Effect of drying methods on the physiochemical characteristics of the**

328   **microcapsules**

17

329   Physiochemical properties (oxidative stability, surface oil, total oil, microencapsulation

330   efficiency and morphological analysis through SEM) of spray and freeze dried tuna oil

331   microcapsules produced by microencapsulating with WPI-GA complex coacervates are

332   discussed in this section.

333   The *OSI* values of blank tuna oil (control), freeze dried and spray dried solid

334   microcapsules are presented in Fig. 6. These *OSI* data suggest that both freeze and spray

335   dried tuna oil microcapsules exhibited significantly (p <0.05) better oxidative stability

336   compared to the control (OSI = 3.1 h). The OSI value for freeze dried sample was 13.2 h

337   compared to 22.1 h for spray dried sample implying that the freeze dried microcapsules

338   were less stable against oxidation compared to the spray dried ones. This may be due to

339   the highly porous structure of the freeze dried powder.[34] The porous structure makes it

340   easier for oxygen to diffuse through the porous shell structure to access the encapsulated

341   oil and weakens the oxidative stability.[35,36] This relatively poor oxidative stability in

342   freeze dried microcapsules can also be explained by their morphology identified by SEM

343   (Fig. 7B). Freeze dried microcapsules possess irregular shape, are flake-like and have a

344   highly porous structure.

345   The spray dried microcapsules were found to be significantly more stable (p < 0.05)

346   against oxidation, as compared to freeze dried microcapsules, even though much higher

347   temperature was used in the spray drying process. This relatively high *OSI* of spray dried

348   microcapsules can be attributed to the compact structure of the spray dried solid

349   microcapsules (Fig. 7A). The outer topography of the spray dried particles indicates that

350   there is no shell rupture and the shell is much less porous compared to freeze dried

351   microcapsules. The absence of pores/ cracks on the particle surface is very important for

352   preventing the inward diffusion of oxygen and hence for better protection of the

353   encapsulated oil. The SEM micrograph shows that the spray dried microcapsules have

354   uniform size distribution below 5 μm (based on 100 microcapsules) with wrinkled

355   spherical shape, resulting from the protein in the wall material. The wrinkled surface is

356   typical characteristics of spray dried powders with protein in the matrix.[37-39] Moreover,

357   this significantly enhanced oxidative stability for spray dried microcapsules compared to

358   freeze dried ones is partly due to lower overall surface area and lower surface oil content.

359   The surface oil and total oil contents, and microencapsulation efficiency of the freeze and

360   spray dried microcapsules, are shown in Fig. 8. The freeze dried solid microcapsules had

361   higher surface oil content (11.41%) as shown in Fig. 8, and lower microencapsulation

362   efficiency. Surface oil is the unencapsulated oil found on the surface of the

363   microparticles, and can trigger lipid oxidation and is a result of lower oil encapsulation

364   efficiency.[40] The microencapsulation efficiency of freeze dried microcapsules was 72.95

365   %, which is significantly (p<0.05) lower than that of spray dried microcapsules (Fig. 8).

366   Similar result was also observed by Quispe-Condori et al.[41] when investigating the

367   microencapsulation efficiency of freeze dried and spray dried flaxseed oil microcapsules.

368

369   **4. Conclusions**

370   The complex coacervation process between WPI and GA was optimised in terms of pH

371   and WPI-to-GA ratio. The WPI-GA complex coacervates were used to microencapsulate

372   omega-3 rich tuna oil. Solid microcapsules of tuna oil were produced through spray

373   drying and freeze drying. The optimal complexation pH and WPI-to-GA ratio were found

374   to be 3.75 and 3:1, respectively. The spray dried microcapsules were found to be more

375   stable against oxidation compared to those prepared by freeze drying. The spray dried

376   microcapsules had the advantage of higher microencapsulation efficiency and lower

377   surface oil content compared to the freeze dried samples. We conclude that WPI-GA

378   complex coacervates can effectively microencapsulate omega-3 rich oils such as tuna oil

379   and the solid microcapsules produced using spray drying will have high encapsulation

380   efficiency and stability against oxidation.

387

Food & Function Accepted Manuscript

388   **References**

389   1 R. K. McNamara and S. E. Carlson, *Prostaglandins, Leukotrienes and Essential Fatty*

390   *Acids,* 2006, **75**, 329-349.

391   2 D. P. Rose and J. M. Connolly, *Pharmacol. Ther.,* 1999, **83**, 217-244.

392   3 H. C. Bucher, P. Hengstler, C. Schindler and G. Meier, *Am. J. Med.,* 2002, **112**, 298-

393   304.

394   4 P. M. Kris-Etherton, W. S. Harris and L. J. Appel, *Arterioscler. Thromb. Vasc.*

395   *Biol.,* 2003, **23**, e20-e30.

396   5 T. K. Dey, S. Ghosh, M. Ghosh, H. Koley and P. Dhar, *Food Res. Int.,* 2012, **49**, 72-79.

397   6 R. J. Hsieh and J. E. Kinsella, *Adv. food nutr. res .,* 1989, **33**, 233-341.

398   7 E. N. Frankel, *Chem. Phys. Lipids.,* 1987, **44**, 73-85.

399   8 K. Heinzelmann and K. Franke, *Colloids and Surfaces B: Biointerfaces,* 1999, **12**, 223-

400   229.

401   9 J. Velasco, C. Dobarganes and G. Márquez-Ruiz, *Grasas Aceites,* 2003, **54**, 304-314.

402   10 V. Ducel, J. Richard, P. Saulnier, Y. Popineau and F. Boury, *Colloids Surf.*

403   *Physicochem. Eng. Aspects,* 2004, **232**, 239-247.

404 11 C. J. Barrow, C. Nolan and Y. Jin, *Lipid technology,* 2007, **19**, 108-111.

405 12 J. N. de Wit, *J. Dairy Sci.,* 1998, **81**, 597-608.

406 13 B. Adhikari, T. Howes, A. K. Shrestha and B. R. Bhandari, *Chemical Engineering and*

407 *Processing: Process Intensification,* 2007, **46**, 420-428.

408 14 C. Butstraen and F. Salaün, *Carbohydr. Polym.,* 2014, **99**, 608-616.

409 15 S. Nie, C. Wang, S. W. Cui, Q. Wang, M. Xie and G. O. Phillips, *Food*

410 *Hydrocoll.,* 2013, **31**, 42-48.

411 16 A. M. Islam, G. O. Phillips, A. Sljivo, M. J. Snowden and P. A. Williams, *Food*

412 *Hydrocoll.,* 1997, **11**, 493-505.

413 17 N. Garti and M. E. Leser, *Polym. Adv. Technol.,* 2001, **12**, 123-135.

414 18 F. Weinbreck, M. Minor and C. De Kruif, *J. Microencapsul.,* 2004, **21**, 667-679.

415 19 W. Zhang, C. Yan, J. May and C. J. Barrow, *Agro Food Industry Hi-Tech,* 2009, **20**,

416 18-21.

417 20 S. Ponsart and D. J. Burgess, *European Journal of Pharmaceutical Sciences,* 1996, **4,**

418 76.

419   21 C. Anandharamakrishnan, C. D. Rielly and A. G. Stapley, *Dairy Science &*

420   *Technology,* 2010, **90**, 321-334.

421   22 A. Gharsallaoui, G. Roudaut, O. Chambin, A. Voilley and R. Saurel, *Food Res.*

422   *Int.,* 2007, **40**, 1107-1121.

423   23 H. Espinosa-Andrews, K. E. Enríquez-Ramírez, E. García-Márquez, C. Ramírez-

424   Santiago, C. Lobato-Calleros and J. Vernon-Carter, *Carbohydr. Polym.,* 2013, **95**, 161-

425   166.

426   24 Y. Yuan, Z. Wan, X. Yang and S. Yin, *Food Res. Int.,* 2014, **55**, 207-214.

427   25 B. W. Mathäus, *Journal of the American Oil Chemists' Society,* 1996, **73**, 1039-1043.

428   26 M. W. Läubli and P. A. Bruttel, *Journal of the American Oil Chemists'*

429   *Society,* 1986, **63**, 792-795.

430   27 S. Liu, N. Low and M. T. Nickerson, *J. Am. Oil Chem. Soc.,* 2010, **87**, 809-815.

431   28 B. Chen, H. Li, Y. Ding and H. Suo, *LWT-Food Science and Technology,* 2012, **47**,

432   31-38.

433   29 E. Dickinson, *Food Hydrocoll.,* 2003, **17**, 25-39.

434 30 C. G. de Kruif, F. Weinbreck and R. de Vries, *Current Opinion in Colloid & Interface*

435 *Science,* 2004, **9**, 340-349.

436 31 A. Ye, *Int. J. Food Sci. Tech.,* 2008, **43**, 406-415.

437   32 A. Kulmyrzaev, M. P. C. Sivestre and D. J. McClements, *Food Res. Int.,* 2000, **33**,

438 21-25.

439 33 Y. Yeo, E. Bellas, W. Firestone, R. Langer and D. S. Kohane, *J. Agric. Food*

440 *Chem.,* 2005, **53**, 7518-7525.

441 34 S. S. Sablani, M. S. Rahman, M. K. Al-Kuseibi, N. A. Al-Habsi, R. H. Al-Belushi, I.

442 Al-Marhubi and I. S. Al-Amri, *J. Food Eng.,* 2007, **80**, 68-79.

443 35 M. S. Rahman, O. S. Al-Amri and I. M. Al-Bulushi, *J. Food Eng.,* 2002, **53**, 301-313.

444 36 P. N. Ezhilarasi, D. Indrani, B. S. Jena and C. Anandharamakrishnan, *J. Food*

445 *Eng.,* 2013, **117**, 513-520.

446 37 A. Soottitantawat, F. Bigeard, H. Yoshii, T. Furuta, M. Ohkawara and P.

447 Linko, *Innovative Food Science & Emerging Technologies,* 2005, **6**, 107-114.

448 38 R. V. Tonon, C. R. F. Grosso and M. D. Hubinger, *Food Res. Int.,* 2011, **44**, 282-289.

449 39 Y. Y. Xu, T. Howes, B. Adhikari and B. Bhandari, *Drying Technol,* 2013, **31**, 1939-

450 1950.

451 40 N. Hardas, S. Danviriyakul, J. L. Foley, W. W. Nawar and P. Chinachoti, *LWT - Food*

452 *Science and Technology,* 2000, **33**, 506-513.

453 41 S. Quispe-Condori, M. D. A. Saldaña and F. Temelli, *LWT - Food Science and*

454 *Technology,* 2011, **44**, 1880-1887.

455

456

457

458

459

460

461

462

463

464

483   carrying out complex coacervation at pH 6.0, (E) Coacervate microcapsules not showing

484   (blue) oil droplets at pH 3.75 and (F) Coacervate microcapsules showing (blue) oil

485   droplets at pH 3.75.

486   Fig. 6: Oxidative stability index of microcapsules measured by accelerated oxidation test

487   using Rancimat^{TM}.

488   Fig. 7: SEM micrographs of spray dried (A) and freeze dried microcapsules (B). P

489   indicates pores in the shell.

490   Fig. 8: Surface oil (SO), total oil (TO) and microencapsulation efficiency (ME) of spray

491   dried and freeze dried complex coacervate microcapsules.

492

493

494

495

496

497

498

499

500

501   Table 1: Omega-3 fatty acids composition of tuna oil

Omega-3 fatty acids	Percentage (%)
16:3w3	0.97
18:3w3 ALA	0.40
18:4w3	0.60
20:4w3	0.46
20:5w3 EPA	5.98
22:5w3	1.20
22:6w3 DHA	29.42
Sum Omega-3 –PUFAS	39.03

502   NuMega Ingredients Ltd. (Victoria, Australia)

503

504

505

506
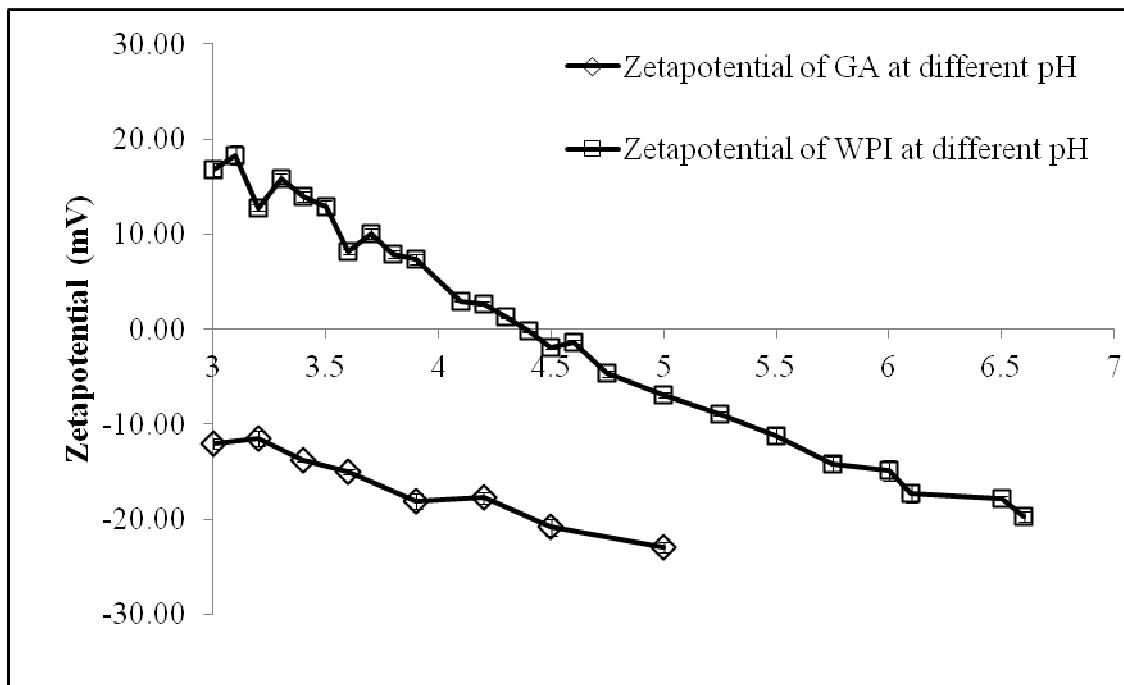
Fig. 1A: Effect of pH on zetapotential of WPI and GA dispersions.
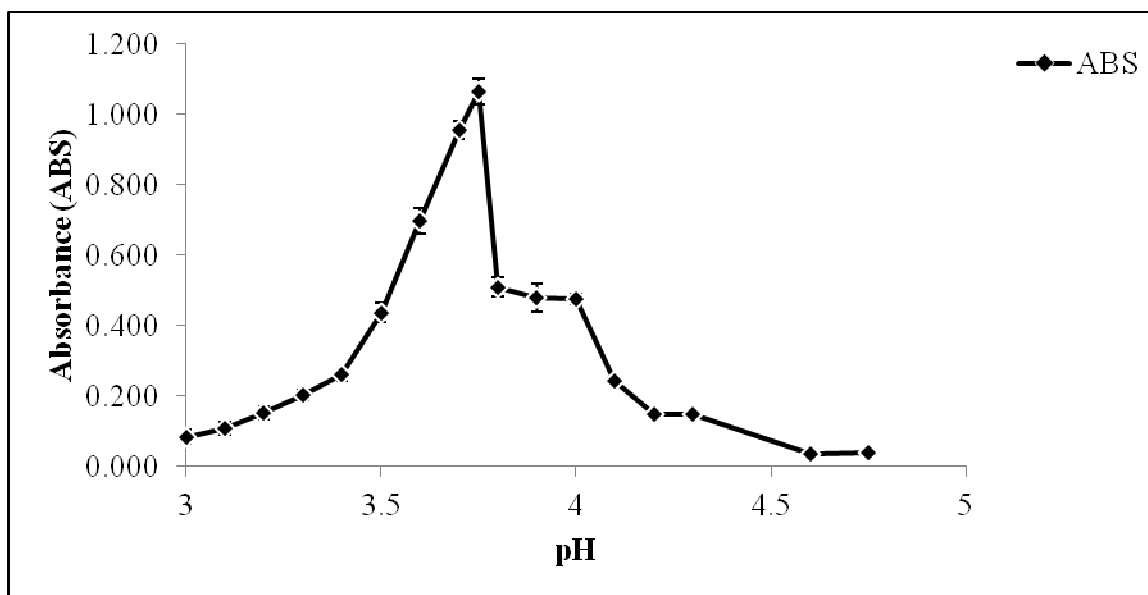
Fig. 1B: Turbidity values of WPI and GA mixed dispersions at different pH values at WPI to GA ratio = 3:1.
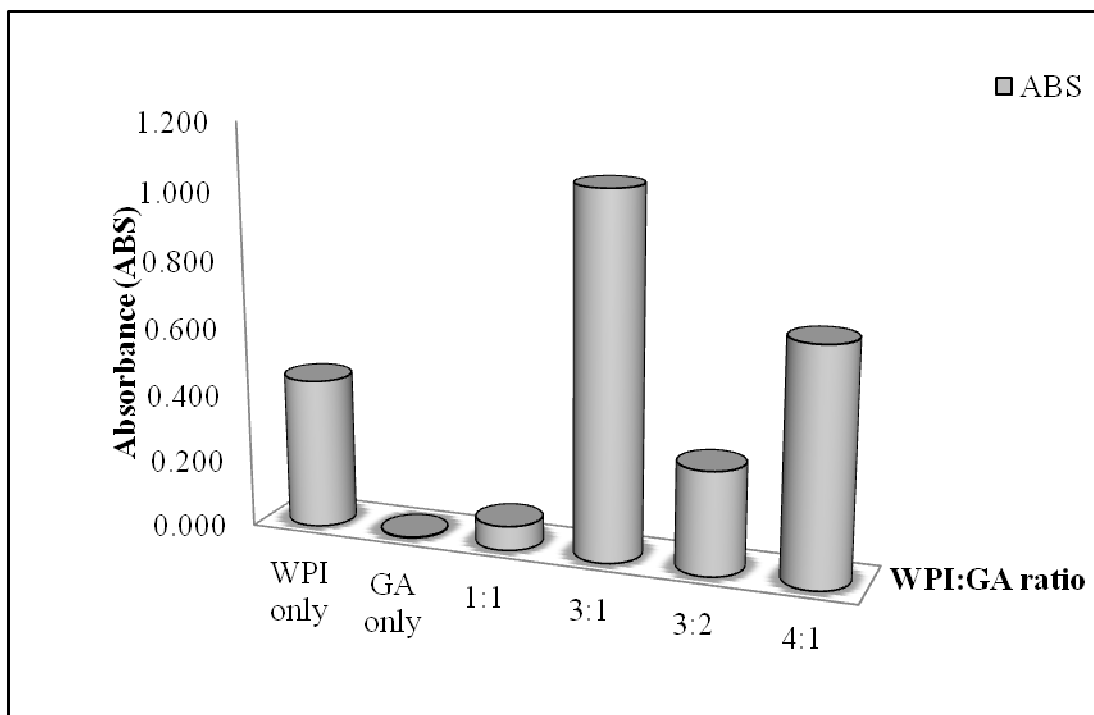
512

513   Fig. 2A: Turbidity values at different WPI to GA ratios.
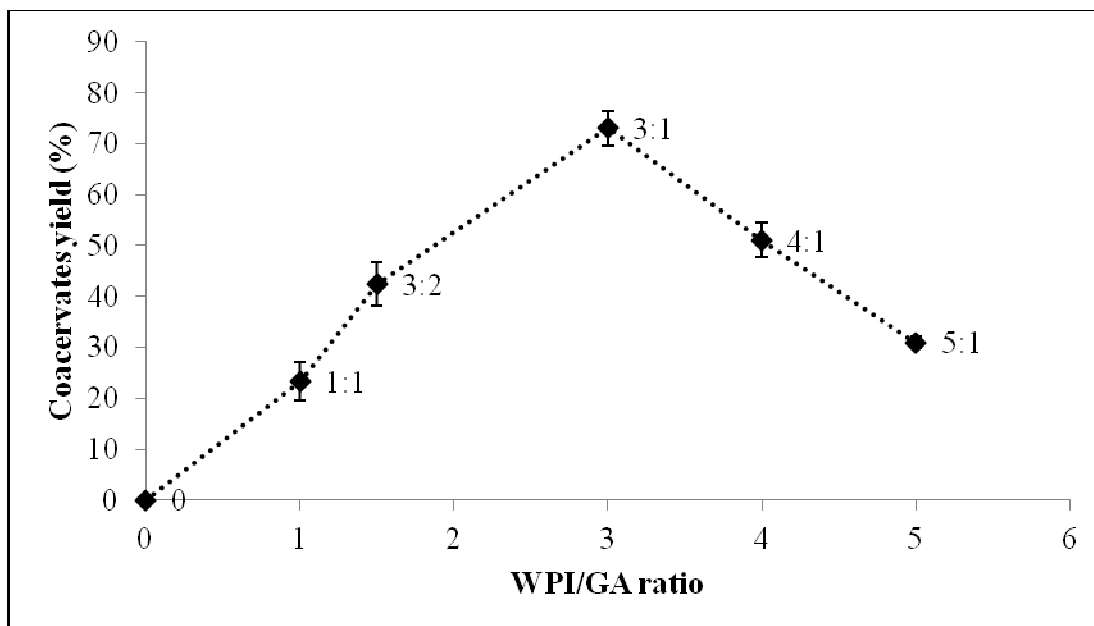
514

515   Fig. 2B: Yield of complex coacervates at different WPI to GA ratios.

516

517

518

519

520
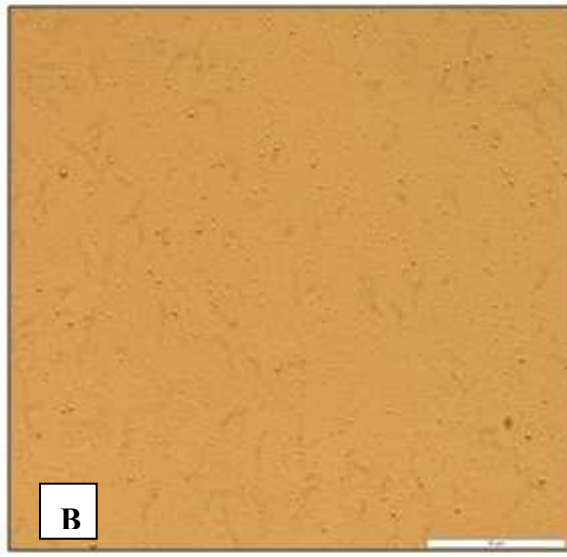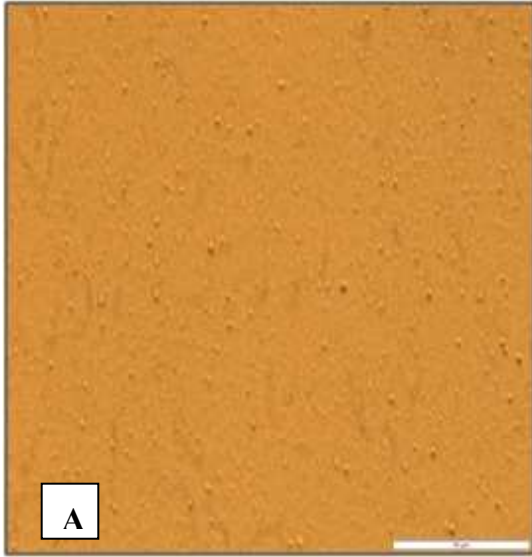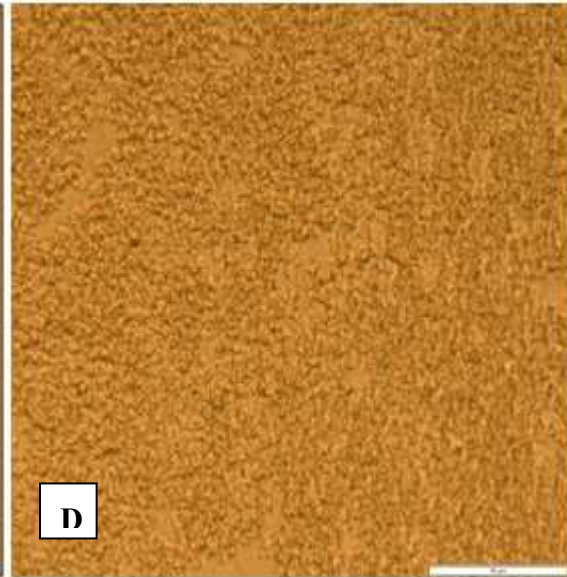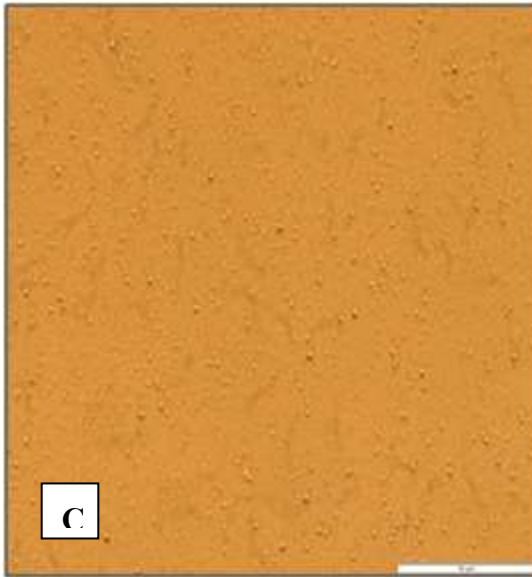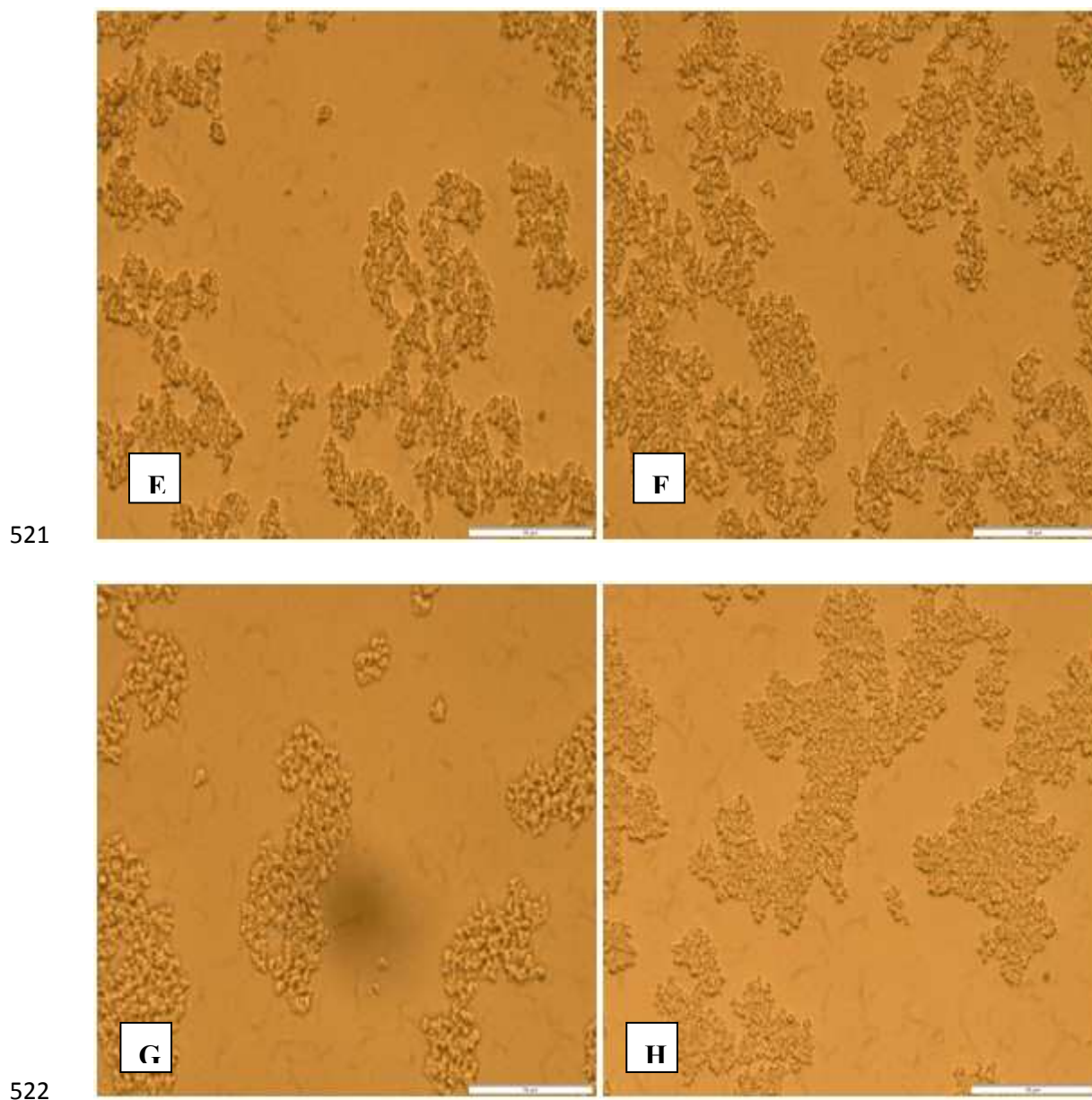
Fig. 3: WPI-GA complex coacervates observed through light microscopy as a function of pH. (A) pH 6.0; (B) pH 5.5; (C) pH 5.0; (D) pH 4.5; (E) pH 4.0; (F) pH 3.8;(G) pH 3.75 and (H) pH 3.75 after cooling, scale bar = 10μm.

526

527

528

33
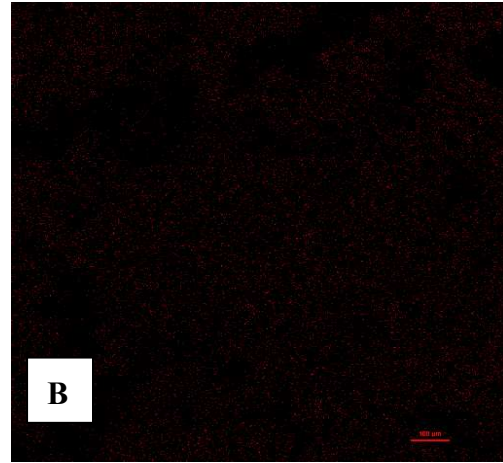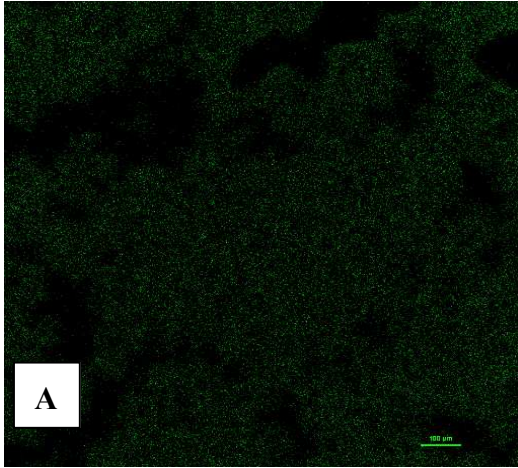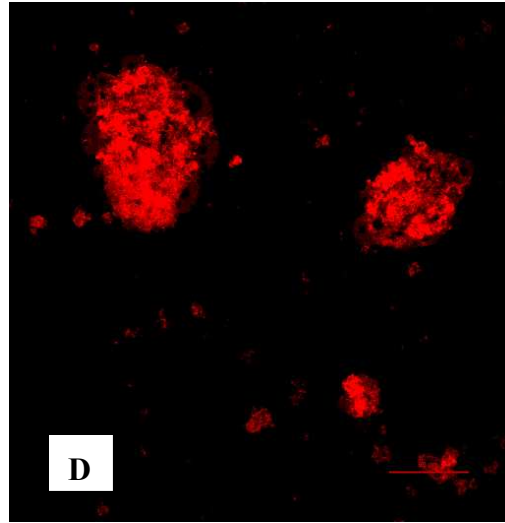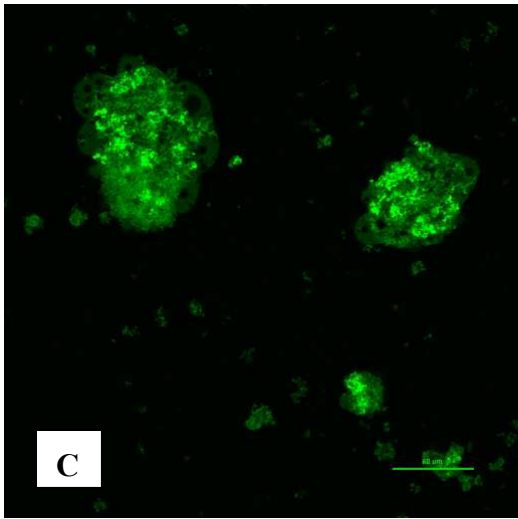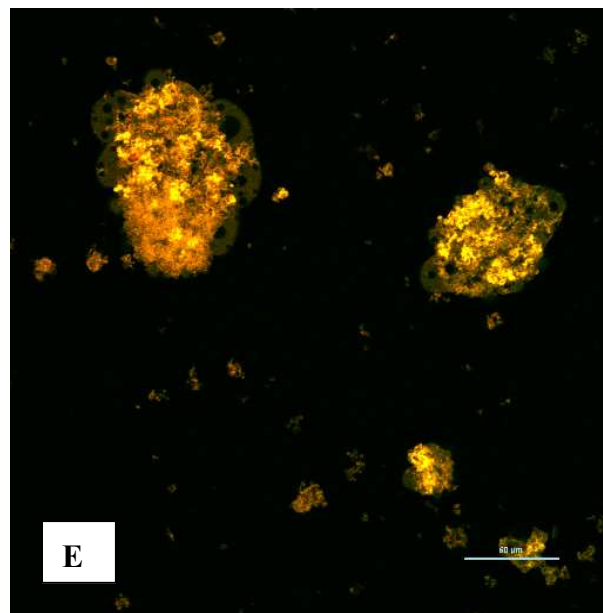
529   Fig. 4: Confocal scanning laser micrographs of (A) WPI (green) in the dispersion before

530   carrying out complex coacervation at pH 6.0, (B) GA (red) in the dispersion before

531   carrying out complex coacervation at pH 6.0 (C) Complex coacervate with labelled WPI

532   (green) at pH 3.75, (D) Complex coacervate with labelled GA (red) at pH 3.75 and (E)

533   Complex coacervates of WPI and GA formed (yellow) at pH 3.75.

534

535

536

537

538

539

540

541

542

543
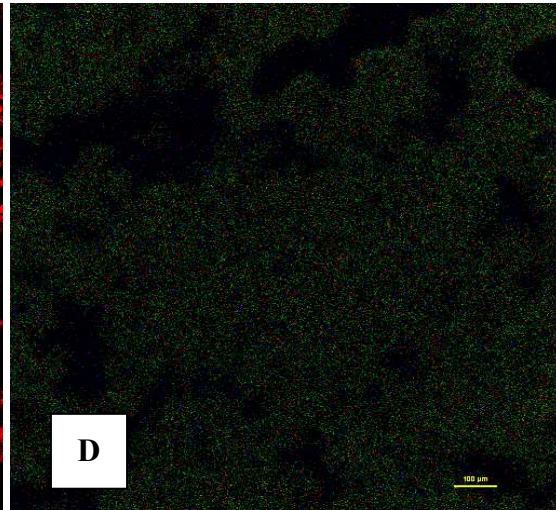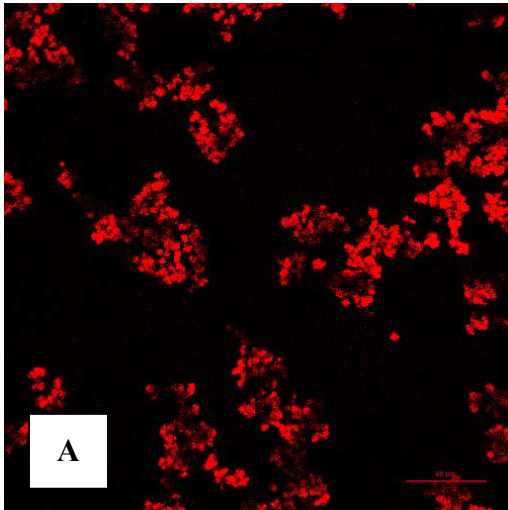
544
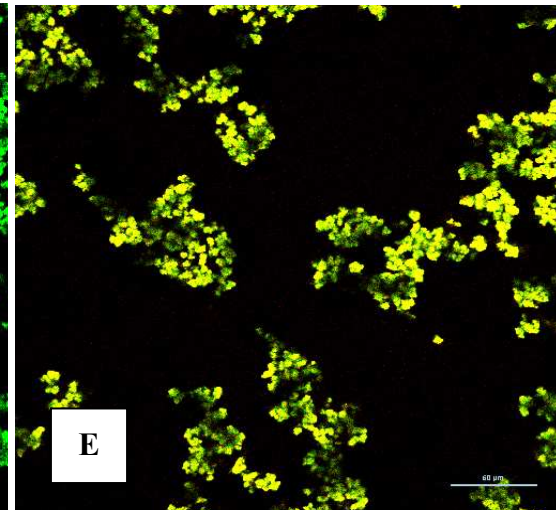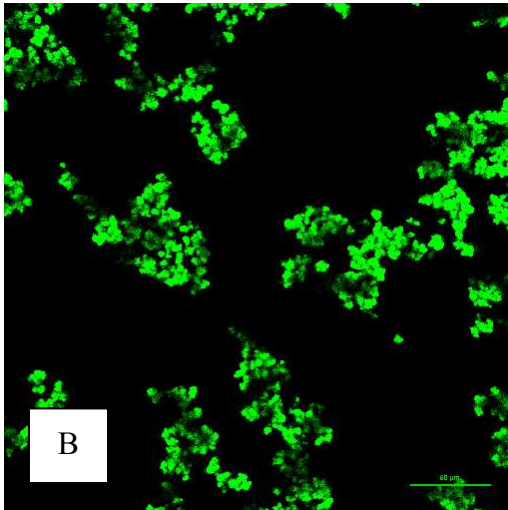
545
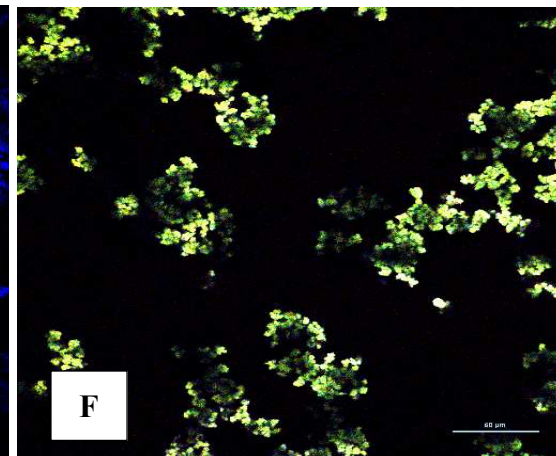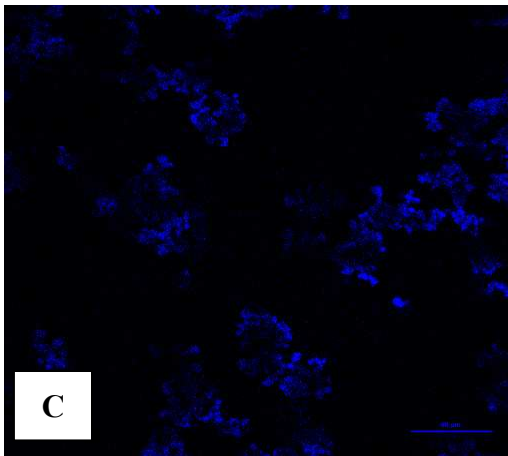
546   Fig. 5: Confocal scanning laser micrographs of (A) GA in the coacervate microcapsules

547   (red), (B)   WPI in the coacervate microcapsules (green), (C) Oil droplets in the

548   coacervate microcapsules (blue), (D) Mixture of WPI (green), GA (red), and oil (blue)

549   before carrying out complex coacervation at pH 6.0, (E) Coacervate microcapsules not

550   showing (blue) oil droplets at pH 3.75 and (F) Coacervate microcapsules showing (blue)

551   oil droplets at pH 3.75.

552

553

554

555

556

557

558
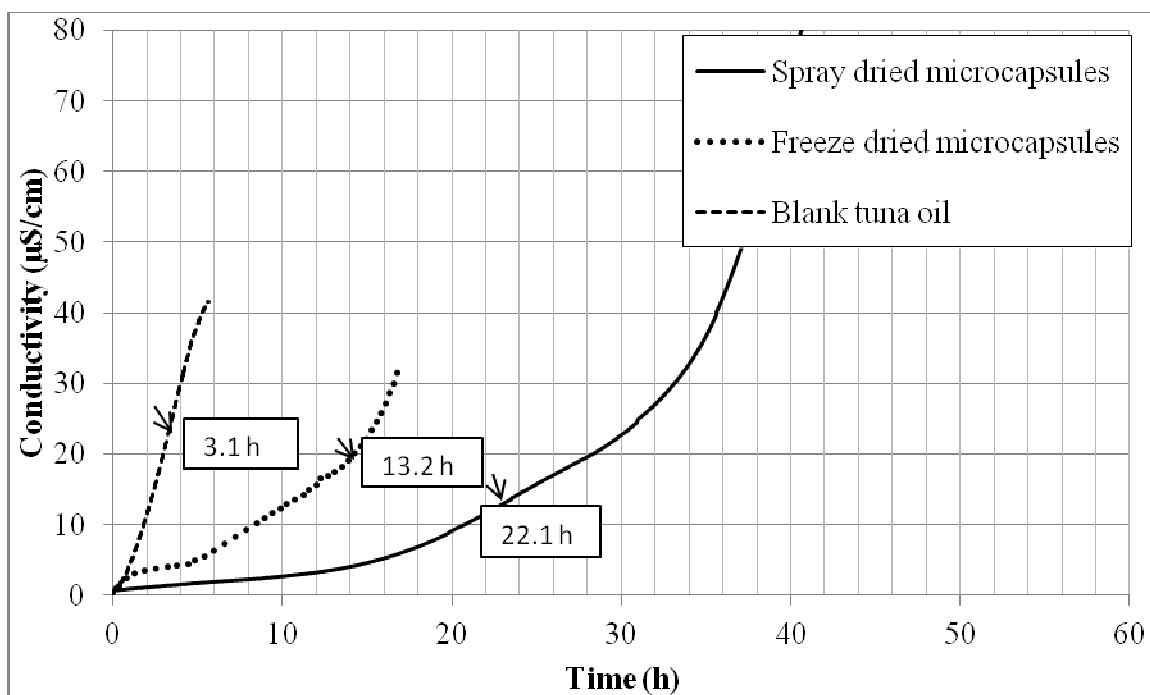
559

560   Fig. 6: Oxidative stability index of microcapsules measured by accelerated oxidation test

561   using Rancimat[TM].

562

563

564

565

566
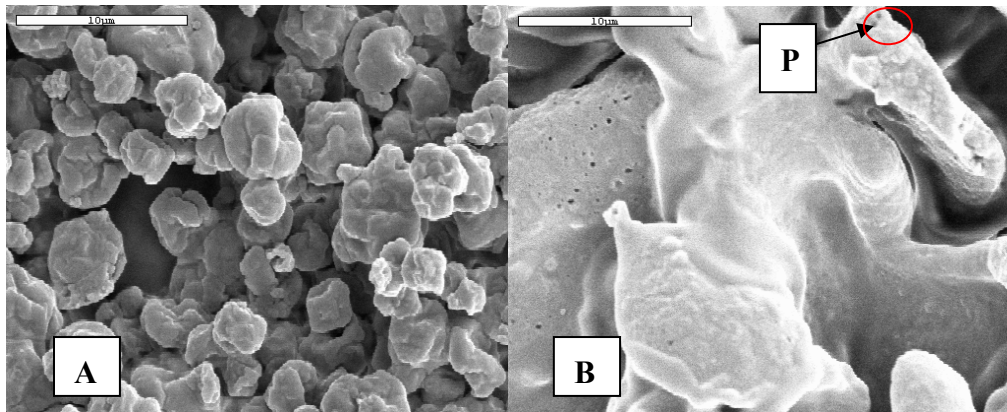
567

568   Fig. 7: SEM micrographs of spray dried (A) and freeze dried microcapsules (B). P

569   indicates pores in the shell.

570

571

572

573

574
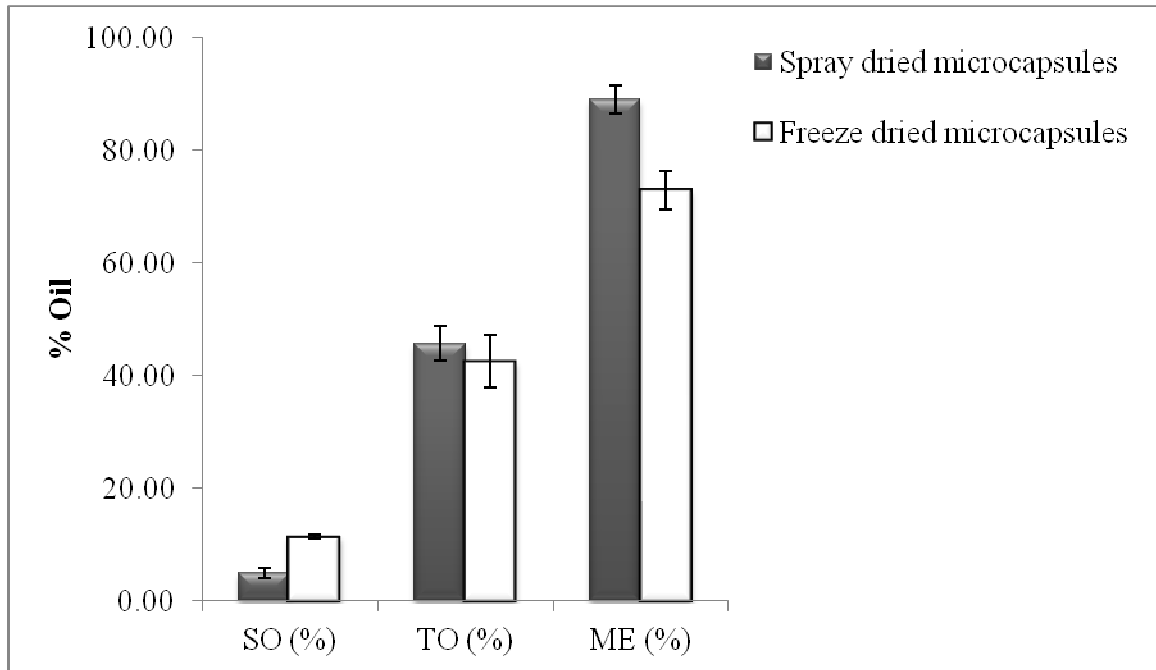
575

576 Fig. 8: Surface oil (SO), total oil (TO) and microencapsulation efficiency (ME) of spray

577 dried and freeze dried complex coacervate microcapsules.

578

579

580

581

582

583

584

585

586